Structural and electronic structure properties of FeSi: the driving force behind the stability of the B20 phase

2001 J. Phys.: Condens. Matter 13 2807

(http://iopscience.iop.org/0953-8984/13/12/305)

INSTITUTE OF PHYSICS PUBLISHING JOURNAL OF PHYSICS: CONDENSED MATTER

J. Phys.: Condens. Matter **13** (2001) 2807–2815 www.iop.org/Journals/cm PII: S0953-8984(01)18798-9

Structural and electronic structure properties of FeSi: the driving force behind the stability of the B20 phase

A I Al-Sharif[1], **M Abu-Jafar**[2] **and A Qteish**[1,3]

[1] Department of Physics, Yarmouk University, Irbid, Jordan
[2] Department of Physics, An-Najah National University, Nablus, Palestine
[3] Department of Physics, Hashemite University, Zarka, Jordan

Received 9 November 2000, in final form 2 February 2001

Abstract

We present the results of a first-principles pseudopotential plane-wave study for the structural properties of the ε-FeSi (B20), NaCl (B1) and CsCl (B2) structures of FeSi. The calculations were performed using the local density and the generalized gradient approximations (LDA and GGA), for the exchange–correlation potential. The electronic structures of the B1 and B2 phases have been similarly investigated. These calculations have enabled us to identify the driving force behind the crystallization of FeSi in the B20 phase. Both the B1 and B2 phases are found to be semimetallic, with the Fermi energy lying in a pseudo-band-gap. The B20 structure is predicted to become unstable with respect to the B2 phase at a moderate pressure, of 13.5 and 10.9 GPa according to the GGA and LDA calculations, respectively.

1. Introduction

At ambient conditions, iron monosilicide crystallizes in the cubic B20 structure (known as ε-FeSi). This system is considered to be a very interesting material for the following reasons. (i) It has unique magnetic properties: the magnetic susceptibility of this system increases rapidly with temperature at low temperatures and has a broad maximum at about 500 K [1]. Several attempts have been made to explain this magnetic behaviour. It has been found that electronic structure calculations, based on the local density approximation (LDA) of the exchange–correlation potential, gave [2] quite small band gap ($\sim$0.1 eV), in good agreement with experiment, but the surrounding bands are not narrow enough to explain the above magnetic properties. Thus, ε-FeSi has been considered as a strongly correlated insulator [3], and going beyond the LDA is necessary to explain its unusual magnetic properties [4]. On the other hand, Jarlborg [5] has shown that such properties can be accounted for using LDA, provided that the thermal disorder effects are included. (ii) The compressibility of ε-FeSi has an important geophysical implication and has been a subject of several investigations. Knittle and Williams [6] have found values for the bulk modulus (B_{eq}) and its pressure derivative (B'_{eq}) of ε-FeSi of 209 GPa and 3.5(4), respectively. These results have led them to conclude that Si might be excluded as a major alloying element for Fe in the outer core of the Earth.

0953-8984/01/122807+09$30.00

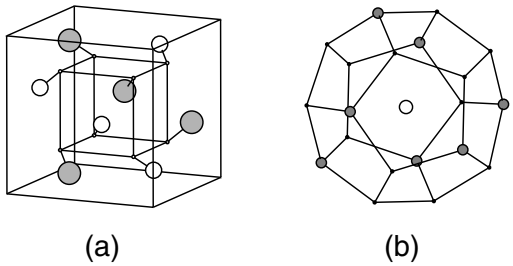

Figure 1. (a) The unit cell of the cubic B20 crystal structure of FeSi. Shaded circles: Si atoms; open circles: Fe atoms. The atoms are connected to their positions in the B1 phase by solid straight lines. The four atoms of each type are at (u, u, u), $(0.5 + u, 0.5 - u, -u)$, $(-u, 0.5 + u, 0.5 - u)$ and $(0.5 - u, -u, 0.5 + u)$, with different values of u for Fe and Si (see text). (b) The regular pentagonal dodecahedron surrounding an Fe atom in the 'ideal' B20 phase, showing the seven Si nearest neighbours.

Unfortunately, the above large value for B_{eq} was not confirmed by the other experimental studies (for a review, see [7]). However, recent theoretical studies [7–10] have provided quite large values for B_{eq}, in excellent agreement with the result of [6]. (iii) When it is epitaxially grown on a Si(111) substrate, FeSi is found to grow in the metallic CsCl (B2) structure [11]. The metallic epitaxial phases of the transition-metal silicides have high potential applications as electrical conductors in Si-based electronic devices. B2-FeSi has a lattice parameter of 2.77 Å, and, hence, a small lattice mismatch with a Si substrate [12]. Moreover, first-principles pseudopotential plane-wave (PP-PW) calculations [9, 10] have found that the equilibrium total energy, E_{tot}, of B2-FeSi is slightly higher than that of ε-FeSi.

The B20 phase has space group $P2_13$, with eight atoms per unit cell. This structure can be considered as a distorted NaCl (B1) structure, where the atoms are moved from their positions in the B1 structure along the [111] directions, see figure 1(a). The B20 structure can be fully determined by three structural parameters: the lattice parameter, a, and two internal parameters, u and v, which determine the Fe and Si atomic positions in the unit cell, respectively. Another important feature to note is that each of the Fe and Si atoms in the 'ideal' B20 structure has seven nearest neighbours of the other type. Interestingly, the neighbouring atoms lie in seven out of the 20 vertices of a regular pentagonal dodecahedron [13], as shown in figure 1(b). In this 'ideal' B20 structure, $u = -v = 1/4\tau = 0.154\,51$, and the dodecahedron edge length is a/τ^2. Here, τ is known as the golden ratio, which is equal to $(1+5^{1/2})/2$. However, the actual values of u and v differ from the above ideal values (experimentally, they are 0.1363(5) and $-0.1559(5)$, respectively), which leads to a splitting of the seven equivalent nearest-neighbour distances into three, three and one. Hereafter, the actual B20 form will be referred to as B20 phase. Recently, Vočaldo, Price and Wood (VPW) [10] have found that it is this relaxation which stabilizes the B20 phase with respect to the B1 structure.

On the other hand, Mattheiss and Hamann [2] have found that the LDA energy difference between the B20 and B1 phases of FeSi is very large (about 1.6 eV/formula unit). From the calculated density of states (DOS) of the B1 phase and the location of the Fermi energy, they concluded that the relaxation associated with the B1 to B20 phase transition is not due to Fermi-surface effects. This conclusion is consistent with the fact that the transition-metal monosilicides that crystallize in the B20 phase (RuSi, MnSi, CoSi and CrSi) have different electrical properties: CrSi and MnSi are metals, CoSi is a semimetal, while FeSi is a narrow-gap semiconductor. All these monosilicides have internal relaxation parameters close to that of FeSi. It has been shown that the electrical properties of the above monosilicides can be

explained [14] by assuming a fixed density of states for all these systems, and so they differ because of the difference in the number of valence electrons. Thus, the position of the Fermi energy has negligible influence on the internal relaxation of these monosilicides. VPW [10] have suggested that the B20 phase is stabilized by the degree of covalency allowed by its atomic arrangement. However, no systematic study of the bonding in the B20, B1 and B2 phases has been made. Thus, the driving force behind the stability of the B20 phase of the above monosilicides is still an open problem.

The main purpose of this work is to shed more light on the driving mechanisms behind the stability of the B20 phase of FeSi, relative to the B1 and B2 structures. To this end, we have performed PP-PW calculations for the structural properties of the above three phases, and the electronic structure of the last two. The structural properties of the 'ideal' B20 form have also been similarly investigated. Two approximations for the exchange–correlation potential have been utilized: the local density and generalized gradient approximations (LDA and GGA). Our results will be analysed and discussed in comparison with the available experimental data and other theoretical results.

The other computational details are as follows. The Kohn–Sham equations were solved using the conjugate gradient methods of [15] and [16]. The integration over the first Brillouin zone was performed using the special point technique and a regular $8 \times 8 \times 8$ Monkhorst–Pack (MP) mesh [17] for the four structures considered. Both of the B20 phases considered were treated as semiconductors, while the other two structures were treated as metals. For the B1 and B2 forms, a Gaussian broadening of the eigenvalues has been used, with a Gaussian smearing parameter of 0.4 eV. It has been found that the corrected (see [18]) E_{tot} is independent of the smearing parameter used, around the adopted value, suggesting that an excellent convergence has been reached. When comparing our present results with those reported in [7] for the B20 phase, obtained by using a $4 \times 4 \times 4$ MP mesh, one can safely conclude that an excellent convergence has also been reached in this case. The rest of the computational details as well as the Fe and Si pseudopotentials used are as described in [7].

2. Results and discussion

2.1. Relative stability and structural parameters

The structural properties of the four considered phases of FeSi were determined by calculating E_{tot} at seven or eight different volumes (V) around the equilibrium one, and fitting the obtained values to the Murnaghan equation of state. In the case of the B20 phase, the optimal internal parameters were determined for each of the considered values of V. The fitted E_{tot} versus V curves for the four considered phases of FeSi, calculated using LDA and GGA, are shown in figure 2. It is evident that the B20 phase is the most stable one, which is consistent with the fact that this phase is the ground state structure of FeSi. The LDA calculations show that the ground-state E_{tot} of the B1, B2 and 'ideal' B20 forms of FeSi are higher than that of the B20 phase by 1.617, 0.067 and 0.125 eV/formula unit, respectively, whereas, the corresponding GGA results are 1.505, 0.087 and 0.128 eV/formula unit. The LDA result for the B1 phase is in excellent agreement with that of Mattheiss and Hamann [2], of 1.60 eV/formula unit, obtained using an LAPW approach. Moreover, the GGA results for both the B1 and B2 phases are also in very good agreement with those of VPW [10], of 1.506 and 0.084 eV/formula unit, obtained using a PP-PW approach and ultra-soft pseudopotentials.

The calculated structural parameters of the ε-FeSi are listed in table 1, together with the available experimental data and other theoretical results. It is evident that our results (obtained using highly optimized PPs) are in excellent agreement with the other PP-PW

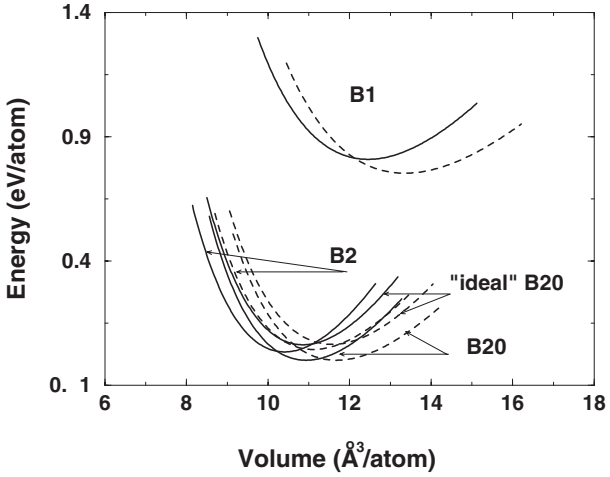

Figure 2. E_{tot} versus V curves of the four considered phases of FeSi. Solid lines: LDA results. Dashed lines: GGA results. In both cases, the zero energy is considered to be the ground state E_{tot} of the B20 phase.

(in which ultra-soft pseudopotentials were used), FP-LAPW and LMTO calculations, and, in turn, the theoretical results are in very good agreement with experiment, except for B_{eq}. The calculated values for B_{eq} are, generally speaking, higher than the experimental ones. The scattering of the experimental results, between 111 and 209 GPa, is quite surprising and can not be explained as due to the pressure ranges considered [7, 10]. On the other hand, the B_{eq} of ε-FeSi has been found to have quite a strong temperature dependence [19]. Thus, the most plausible explanation [10] of the discrepancies in the measured values of B_{eq} is due to the samples studied: small deviations from the 1:1 stoichiometry lead to excess or deficient in the number of valence electrons, which could have significant effects on B_{eq}. It should be noted that Fe_xSi_{1-x} is stable [20] over the composition range from $x = 0.494$ to $x = 0.506$.

The structural parameters of the other three studied phases of FeSi are also shown in table 1. The important features to note are as follows. (i) The calculated and measured values of a_{eq} of the B2 phase show that it has a small lattice mismatch with bulk Si ($a_{eq} = 5.43$ Å), of about 2%. This finding and the above small difference between the ground-state E_{tot} of the B20 and B2 phases provides an explanation for the epitaxial growth of the latter phase of FeSi on Si substrates. (ii) The calculated a_{eq} of the B1 phase is larger than that of the B20 structure. Thus, going from the former to the latter phases does not only involve internal relaxation, but also a reduction in the equilibrium volume per atom. This point will be discussed further below. (iii) The GGA results for a_{eq} for all systems considered are larger than the corresponding LDA values, and the reverse is true for B_{eq}. This is consistent with the well established trend that GGA leads to softer materials than those obtained using LDA.

2.2. Electronic structure of the B1 and B2 phases

In figures 3 and 4 we show the band structure and DOS of the B1 and B2 phases of FeSi, respectively. In the DOS calculations we have used 89 and 165 $\boldsymbol{k}$-points for the B1 and B2 phases, respectively, in the irreducible wedge of the corresponding Brillouin zone. The important features to note are the following. (i) The structure of the DOS and the peak locations

Table 1. Structure properties of the considered four phases of FeSi, see text.

Structure	Structural parameter	LDA	GGA	Experiment
B20	a_{eq} (Å)	4.4388[a],4.38[b],4.41[c],4.43[d]	4.5336[a],4.46[b],4.463[e]	4.48552(3)[f]
	B_{eq} (GPa)	223[a],257[b],255[c],220[d]	195[a],223[b],227[e]	111 to 209[g]
	B'_{eq}	4.58[a]	4.20[a],3.9[d]	3.5(4)[h]
	u(Fe)	0.1355[a]	0.1294[a],0.1367[d]	0.1363(5)[i]
	v(Si)	−0.1596[a]	−0.1598[a],−0.1591[d]	−0.1559(5)[i]
'ideal' B20	a_{eq} (Å)	4.429[a]	4.523[a],4.456[e]	—
	B_{eq} (GPa)	240.9[a]	202.9[a],224[e]	—
	B'_{eq}	4.06[a]	4.17[a],4.5[e]	—
B1	a_{eq} (Å)	4.636[a]	4.671[a],4.671[e]	—
	B_{eq} (GPa)	173[a]	144[a],163[e]	—
	B'_{eq}	4.09[a]	4.05[a],3.9[e]	—
B2	a_{eq} (Å)	2.751[a],2.72[b],2.72[c]	2.810[a],2.77[b],2.768[e]	2.77[j]
	B_{eq} (GPa)	251[a],263[b],270[c]	204[a],221[b],226[e]	222[j]
	B'_{eq}	4.00[a]	5.21[a],5.4[e]	—

[a] Present work: PP-PW calculations, using highly optimized pseudopotentials.
[b] [9]: PP-PW calculations, using ultra-soft pseudopotentials.
[c] [8]: LMTO calculations.
[d] [9]: FP-LAPW calculations.
[e] [10]: PP-PW calculations, using ultra-soft pseudopotentials.
[f] [21].
[g] See [7], and references therein.
[h] [6].
[i] [22].
[j] [23].

agree well with those of [2] for the B1 phase, and [23] and [24] for the B2 structure. (ii) Both B1 and B2 phases of FeSi are semimetals, with the Fermi energy lying in a pseudo-gap. This has led Mattheiss and Hamann [2] to conclude that the internal relaxation of the B1 form which leads to the B20 phase is not driven by Fermi surface effects, such as charge-density-wave distortions or Peierls transitions. This issue will be discussed in some detail in the next subsection. (iii) In the DOS of the B1 phase (figure 3), the peak just below the Fermi energy is due to the flat band states around the L-point and along the X–W-direction. The peak centred at about −3 eV originates from flat band states around the L-point and along the Γ–K-direction. The peak centred at about −5.5 eV is due to the states around the K-points. The peak just above the Fermi energy is due to the flat band states along the X–W-direction. (iv) In the case of the DOS of the B2 phase (figure 4), the main peaks centred at about −3 eV are due to the highest occupied states around the M-, X- and Γ-points, while that at about −6 eV is due to those around the R-point. The peak just above the Fermi energy is due to the flat band states around the X-point.

2.3. Driving mechanism behind the stability of the B20 phase

The crystallization of FeSi in the B20 phase has been recently discussed, by inspecting the electronic structure of this phase in comparison with those of the B1 and B2 forms [2, 10]. In this work we have adopted a different and more direct approach, through inspecting the individual contributions to E_{tot}. We have found that it is more convenient to separate E_{tot} as follows:

$$E_{tot} = E_{elec} + E_{Ewald}.$$

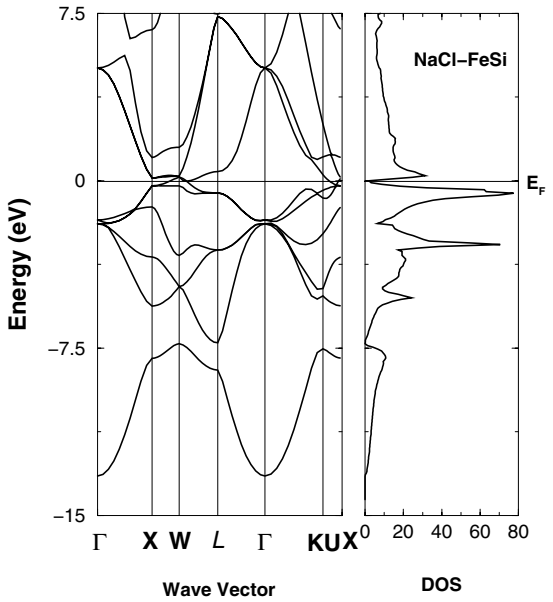

Figure 3. The band structure, along the high-symmetry directions of the FCC Brillouin zone, and the density of states of the B1 phase of FeSi.

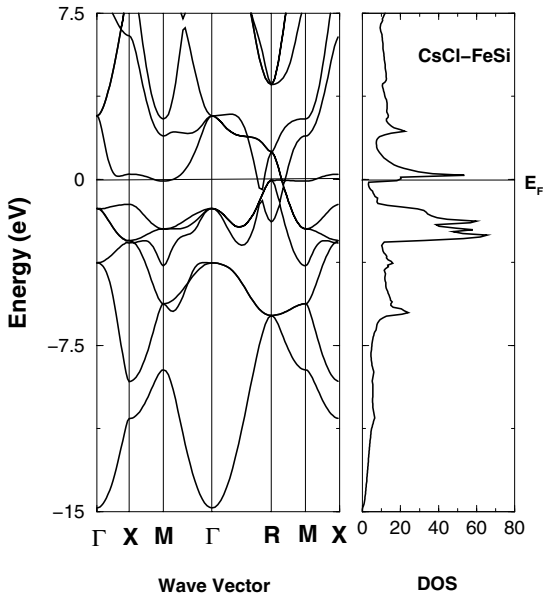

Figure 4. As in figure 3, but for the B2 phase of FeSi.

Here, E_{elec} takes care of the electron–electron and electron–ion interaction energies, and E_{Ewald} is the Ewald energy, which represents the ion–ion interaction energy. It is obvious that the first term depends on the electronic charge density distribution (or chemical bonding), while the latter depends only on the ionic configuration. The differences between E_{tot}, E_{elec} and E_{Ewald}

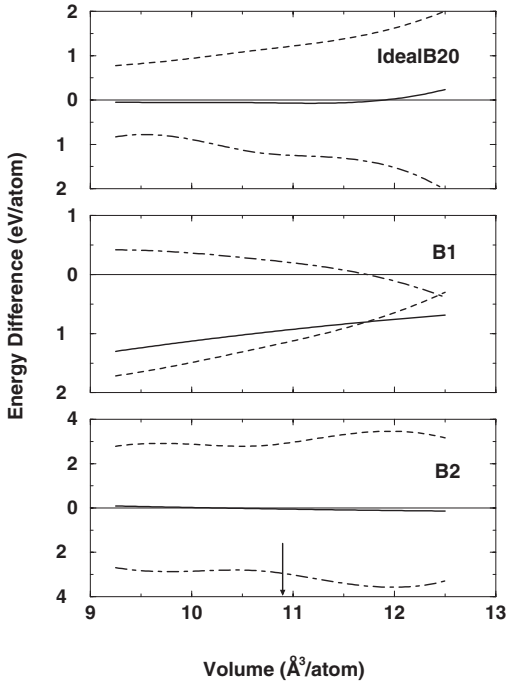

Figure 5. The energy differences between the B1, B2 and 'ideal' B20 phases of FeSi and the corresponding B20 phase, as functions of volume per atom. Solid line: total energy (E_{tot}). Dashed–dotted lines: electronic energy (E_{elec}). Dashed lines: Ewald energy (E_{Ewald}). The negative energy difference means that the corresponding energy is lower in the B20 phase. The arrow indicates the position of the equilibrium volume of the B20 phase.

of the 'ideal' B20, B1 and B2 phases and the corresponding quantities of the B20 structure, as functions of volume, are shown in figure 5. Here, only the LDA results are shown, and the GGA ones would lead to the same conclusions. The most important features to note from figure 5 are the following.

First, the E_{Ewald} of the B20 structure is significantly lower (by about 1.15 eV/atom, at V_{eq} of this phase) than that of the B1 phase over the V-range of interest, whereas E_{elec} is lower in the B1 phase over most of the V-range considered, and it becomes higher than that of the B20 phase above $V = 11.8$ Å^3/atom. Moreover, the magnitude of ΔE_{elec} in this case is much smaller than that of ΔE_{Ewald}. This means that the internal relaxation of the B1 phase, which leads to the B20 form, is driven by ΔE_{Ewald}. This finding is consistent with the conclusion of Mattheiss and Hamann [2] that the above relaxation is not driven by Fermi surface effects. Finally, by going to smaller volumes one observes that the rate of the reduction of ΔE_{Ewald} is larger that of the increase of ΔE_{elec}. This explains why the B20 phase has smaller V_{eq} than that of the B1 form.

Second, the ΔE_{Ewald} of the B2 phase is large and positive over the V-range considered, which shows that E_{Ewald} of this structure is lower than that of the B20 phase. It is also interesting to note that ΔE_{Ewald} is almost fully compensated by a large and negative ΔE_{elec}, leading to only very small relative stability between the B2 and B20 phases. Thus, this shows that, in this case, it is the chemical bonding of the B20 phase which stabilizes the B20 phase with respect to the B2 one.

Third, the E_{Ewald} of the 'ideal' B20 structure is also lower than that of the B20 phase, and the ΔE_{Ewald} is largely compensated by ΔE_{elec}. Around V_{eq} of the B20 phase, the 'ideal' B20 has higher energy than the B2 phases. These results are consistent with the conclusion of VPW [10] that the B20 phase is stabilized with respect to the B2 one by this further internal relaxation, which takes the 'ideal' B20 form to the real one. This relaxation is driven by electronic charge density redistribution, which leads to stronger chemical bonding in the B20 form.

The large magnitude of ΔE_{Ewald} between both the B1 and B2 phases of FeSi and the corresponding B20 structure can be justified as follows. The internal relaxation which takes the B1 phase into the B20 structure is quite large, see figure 1(a), which leads to a large difference between their ionic configurations. At V_{eq} of the B20 form, the B1 phase has six nearest neighbours (nns) of the other type at a distance of 2.2428 Å, and 12 second nns (nnns) of the same type at a distance of 3.1714 Å, whereas in the B20 form each Si or Fe atom has seven nns of the other type at 2.2701(1), 2.3494(3) and 2.5117(3) Å; each Si and Fe has six nnns (of the same type) at 2.7746 and 2.7505 Å, respectively. Here, the experimental values of a_{eq}, u and v of the B20 phase (see table 1) have been utilized. Moreover, in the B2 phase, at the above volume per atom, each Si or Fe atom has eight nns of the other type at 1.7600 Å and six nnns of the same type at 2.8257 Å. Thus, concentrating on the nns and nnns alone, the ionic configuration of the B20 phase lies somewhere between that of the B1 and B2 phases: the number of nns of the B20 phase is intermediate between the other two phases considered, and the nn distances are close to those of the B1 phase, whereas the number of nnns is identical to that of the B2 phase, and the nnn distances are also closer to those of the B2 phase. This explains why the E_{Ewald} of the B20 phase lies between that of B1 and B2 forms, and is appreciably different from them.

We believe that the above arguments for the stabilization of the FeSi in the B20 phase are also valid for the other transition-metal monosilicides that have the same structure. However, further investigations are required to check such a claim. The chemical bonding in the phases of FeSi considered, as well as those of other transition-metal silicides (namely, CoSi and NiSi) are currently under consideration. Moreover, in this work as well as in the other previous work [9, 10] the B2 phase is treated as non-magnetic. Because of the semi-metallic nature of this phase we expect that its magnetic instability, if exists, would be very weak and would not affect our conclusions. This point also requires further investigations.

2.4. Stability of the B2 phase under high pressure

Finally, we discuss the stability of B2-FeSi under high-pressure. Recently, it has been theoretically shown [9, 10] that the B20 phase of FeSi becomes unstable with respect to the B2 form at a moderate pressure (of 13 [9] and 15 [10] GPa). In this work, the transition pressure, p_t, of the B20→B2 transition of FeSi was determined from the constraint of equal static lattice enthalpy. Our LDA and GGA results are of 10.9 and 13.5 GPa, respectively. These results are in excellent agreement with the above theoretical results. One should note, here, that no structural phase transition has been experimentally observed [6] in FeSi under high pressure, up to 49 GPa, and heating the sample at this pressure up to 1500 K. The apparent contradiction between the theoretical and experimental findings can be understood as follows. A continuous B20→B2 transition has to go through the B1 phase [9]: the B20 structure transforms continuously to the B1 phase by changing the internal parameters (see figure 1(a)), and the B1 phase may transform to the B2 form following a Bain path along the [111] direction. Thus, such a transition path would be prohibited by the large energy difference between the B20 and B1 phases.

3. Conclusions

We have presented the results of a first-principles pseudopotential study of the driving mechanisms behind the crystallization of FeSi in the cubic B20 form. This has been done by investigating the structural properties and relative stability of the B20, 'ideal' B20, B1 and B2 phases of FeSi, and the electronic structure properties of the last two. Both LDA and GGA have been utilized for the exchange–correlation potential. Our main results and conclusions can be summarized as follows.

(a) Our results for the structural properties of the above systems are found to be in excellent agreement with the previous theoretical calculations and the available experimental data.
(b) Both B1 and B2 phases of FeSi are found to be semimetals, with the Fermi energy lying in a pseudo-band-gap.
(c) The internal relaxation, which takes the B1 phase into the B20 form, is driven by a large reduction in the Ewald energy per atom, which depends only on the ionic configuration.
(d) With respect to the B2 phase, the B20 structure is stabilized by the bonding characteristics of the latter structure, and the relative stability of these two structures is found to be very small.
(e) The internal relaxation of the 'ideal' B20 phase, which leads to the B20 structure, is also found to be driven by the bonding characteristics of the latter structure, and it is this relaxation which stabilizes the B20 phase with respect to the B2 form.
(f) The B2 phase of FeSi is found to be a thermodynamically stable high-pressure phase, with a transition pressure of the B20→B2 transition of 10.9 and 13.5 GPa, respectively, according to the LDA and GGA calculations.

References

[1] Jaccarino V, Wertheim G K, Wernick J H, Walker L K and Arajs S 1967 *Phys. Rev.* **160** 476
[2] Mattheiss L F and Hamann D R 1993 *Phys. Rev.* B **47** 13 114
[3] Fu C, Krijn M P C M and Doniach S 1994 *Rev.* B **49** 2219
[4] See for example, Anisimov V I, Ezhov S Yu, Elfimov I S, Solovyev I V and Rice T M 1996 *Phys. Rev. Lett.* **76** 1735
[5] Jarlborg T 1999 *Phys. Rev.* B **59** 15 002
[6] Knittle E and Williams Q 1995 *Geophys. Res. Lett.* **22** 445
[7] Qteish A and Shawagfeh N 1998 *Solid State Commun.* **108** 11
[8] Jarlborg T 1995 *Phys. Rev.* B **51** 11 106
[9] Moroni E G, Wolf W, Hafner J and Podloucky R 1999 *Phys. Rev.* B **59** 12 860
[10] Vočaldo L, Price G D and Wood I G 1999 *Acta Crystallogr.* B **55** 484
[11] Degroote S, Vantomme A, Dekoster J, Moons R and Langouche G 1996 *Conf. Proc. ICAME-95* vol 50, ed I Ortalli (Bologna: SIF) p 623
[12] See for example, Fanciulli M *et al* 1999 *Phys. Rev.* B **59** 3675
[13] Wells A F 1956 *The Third Dimension Chemistry* (Oxford: Oxford University Press) pp 12–15
[14] Evangelou S N and Edwards D M 1983 *J. Phys. C: Solid State Phys.* **16** 2121
[15] Teter M P, Payne M C and Allan D C 1989 *Phys. Rev.* B **40** 12 255
[16] Qteish A 1995 *Phys. Rev.* B **52** 14 497
[17] Monkhorst H J and Pack L D 1976 *Phys. Rev.* B **13** 5188
[18] Elsasser C, Fahnle M, Chan C T and Ho K M 1994 *Phys. Rev.* B **49** 13 975
[19] Zinoveva G P, Andreeva L P and Geld P V 1974 *Phys. Status Solidi* a **23** 711
[20] Köster W and Gödecke T 1968 *Z. Metallkd.* **59** 602
[21] Guyot F, Zhang J, Martinez I, Matas J, Ricard Y and Javoy M 1997 *Eur. J. Mineral.* **9** 277
[22] Wood I G, Chaplin T D, David W I F, Hull S, Price G D and Street J N 1995 *J. Phys.: Condens. Matter* **7** L475
[23] von Känel H, Mäder K A, Müller E, Onda N and Sirringhaus H 1992 *Phys. Rev.* B **45** 13 807
von Känel H *et al* 1994 *Phys. Rev.* B **50** 3570
von Känel H, Müller E, Goncalves-Conto S, Schwarz C and Onda N 1996 *Appl. Surf. Sci.* **104/105** 204
[24] Girlanda R, Piparo E and Balzarotti A 1994 *J. Appl. Phys.* **76** 2837